Theoretical extension and experimental demonstration of spectral compression in second-harmonic generation by Fresnel-inspired binary phase shaping

Baihong Li,[1,2,3,*] Ruifang Dong,[1,2,†] Conghua Zhou,[1,2] Xiao Xiang,[1,2] Yongfang Li,[4] and Shougang Zhang[1,2]

[1]*Key Laboratory of Time and Frequency Primary Standards, National Time Service Center, Chinese Academy of Science, Xi'an 710600, China*

[2]*School of Astronomy and Space Science, University of Chinese Academy of Sciences, Beijing, 100049, China*

[3]*College of Sciences, Xi'an University of Science and Technology, Xi'an, 710054, China*

[4]*School of Physics and Information Technology, Shaanxi Normal University, Xi'an, 710062, China*

(Received 10 February 2018; published 7 May 2018)

Selective two-photon microscopy and high-precision nonlinear spectroscopy rely on efficient spectral compression at the desired frequency. Previously, a Fresnel-inspired binary phase shaping (FIBPS) method was theoretically proposed for spectral compression of two-photon absorption and second-harmonic generation (SHG) with a square-chirped pulse. Here, we theoretically show that the FIBPS can introduce a negative quadratic frequency phase (negative chirp) by analogy with the spatial-domain phase function of Fresnel zone plate. Thus, the previous theoretical model can be extended to the case where the pulse can be transformed limited and in any symmetrical spectral shape. As an example, we experimentally demonstrate spectral compression in SHG by FIBPS for a Gaussian transform-limited pulse and show good agreement with the theory. Given the fundamental pulse bandwidth, a narrower SHG bandwidth with relatively high intensity can be obtained by simply increasing the number of binary phases. The experimental results also verify that our method is superior to that proposed in [Phys. Rev. A **46**, 2749 (1992)]. This method will significantly facilitate the applications of selective two-photon microscopy and spectroscopy. Moreover, as it can introduce negative dispersion, hence it can also be generalized to other applications in the field of dispersion compensation.

DOI: 10.1103/PhysRevA.97.053806

I. INTRODUCTION

Selective two-photon microscopy and high-precision nonlinear spectroscopy [1] require the generation of a strong signal at the desired frequency and the suppression of background elsewhere, which are enabled by spectral compression. Many studies have been conducted to achieve this goal by using the method of quantum coherent control. Broers *et al.* [2] first demonstrated spectral focusing in second-harmonic generation (SHG) and two-photon absorption (TPA) using binary amplitude (0, 1) modulation with a structure of Fresnel zone plate. Later, Zheng and Weiner demonstrated the coherent control of SHG and obtained a signal with a high contrast using the idea of binary encoded pulses, which was borrowed from communications technology [3,4]. Moreover, Dantus and coworkers reported various efforts for spectral compression by taking advantage of multiphoton intrapulse interference (MII) [5–14] and demonstrated improved excitation selectivity with outstanding results and efficiencies via binary phase shaping (BPS), based on primary numbers, optimization algorithms [10], and pseudorandom binary phase sequences [14]. However, most of these methods involve more complex algorithms and a large number of binary sequences.

Based on the work by Broers *et al.*, Li *et al.* [15,16] proposed a more advanced scheme, named Fresnel-inspired binary phase $(0, \pi)$ shaping (FIBPS) for spectral compression, in which destructive contributions are sign changed rather than blocked so that all contributions add constructively. However, these earlier works discussed only the theoretical model for spectral narrowing a square-chirped pulse. In this paper, we extend the theory of FIBPS for spectral compression of pulses which can be transformed limited (TL) and in any symmetrical spectral shape (such as Gaussian, Lorentz, and hyperbolic secant). Furthermore, an analogy of our FIBPS method to a Fresnel lens is provided, which can introduce negative dispersion and can also be generalized to applications in the field of dispersion compensation. Finally, we experimentally demonstrate the SHG spectral compression for a Gaussian TL pulse by applying the binary phase sequence to be $N = 13$, 21, and 41, respectively. With $N = 41$, a narrowed bandwidth of only 0.161 nm has been achieved with a compression factor of 11.3 and relative intensity of 56% compared to the TL SHG intensity. Perfect agreements between the experimental results and the theoretical prediction on the bandwidth narrowing have been demonstrated. Further investigation also verifies that our method is superior to that of Broers, especially when the number of binary phase sequences is small. The narrower bandwidth of SHG can be easily achieved by simply increasing the number of binary phase sequences.

The paper is structured as follows. In Sec. II we present the theoretical extension for the spectral compression of SHG by FIBPS. In Sec. III we present the experimental results. We discuss the experimental errors and several possible applications in Sec. IV and close the paper with some concluding remarks in Sec. V.

*baihongli@xust.edu.cn

†dongruifang@ntsc.ac.cn

II. THEORETICAL EXTENSION

The SHG intensity in the frequency domain can be expressed as

$$I_{\mathrm{SHG}}(2\omega) \propto \left| \int E(\omega+\omega')E(\omega-\omega')d\omega' \right|^2, \quad (1)$$

where $E(\omega) = A(\omega)e^{i\phi(\omega)}$, and $A(\omega)$ and $\phi(\omega)$ are the spectral amplitude and phase distribution, respectively. Equation (1) shows that the SHG process occurs only when different pairs of frequency components within the fundamental pulse (FP) add up to a single SHG frequency 2ω. Hence, the spectral compression of SHG can be realized by inducing constructive interference at desired frequency and destructive interference elsewhere through modulating the relative phases between different frequency components within the FP with the pulse-shaping techniques [17].

To obtain the spectral compression, Li *et al.* [15,16] proposed a FIBPS scheme and demonstrate it theoretically for a square-chirped pulse with a phase distribution $\phi(\omega) = \alpha(\omega-\omega_0)^2$, where α is the chirp parameter. If we consider that the FP has a center frequency of ω_0 and a full width of $\Delta\omega$, the SHG intensity can be rewritten as

$$I_{\mathrm{SHG}}[2(\omega_0+\Omega)] \propto \left| \int_{-\Delta\omega/2+\Omega}^{\Delta\omega/2+\Omega} |A(\omega)|^2 e^{i2\alpha\omega^2} d\omega \right|^2, \quad (2)$$

where $\Omega = \omega-\omega_0$ denotes the frequency detuning from the central frequency ω_0 of the FP. The boundary of the nth frequency zone tailored by the FIBPS scheme for an FP spectrum can be expressed as [15,16]

$$\pm\Omega_n = \pm\sqrt{(3/2+2(n-1))\pi/\alpha} \quad (n = 1,2,3\ldots). \quad (3)$$

The total number of frequency zones (binary phases) N is $2n-1$. According to Eq. (3), an FIBPS function can be obtained as follows:

$$FIBPS(\Omega) = \frac{\pi}{2}\left(\prod_n \mathrm{sgn}(\Omega_n - |\Omega|) + 1\right), \quad (4)$$

where sgn is a symbolic function. The above function takes only the value 0 or π for different frequency zones, and the phase difference is π between adjacent frequency zones. By retaining the even frequency zones and introducing the phase π to odd frequency zones, one can add all the contributions constructively rather than merely blocking destructive contributions, as mentioned in Ref [2].

Here, we extend this scheme to a more general case in which the FP is a TL pulse [$\phi(\omega) \equiv 0$] and can be in any shape as long as it is symmetrical about the center frequency, i.e., $E(\omega_0+\Omega)=E(\omega_0-\Omega)$. First, we demonstrate that the FIBPS can introduce a negative quadratic frequency phase factor (negative chirp) for a TL pulse, leading to the same compression result as for a chirped pulse. Therefore, a chirp of the FP is not necessary, and Eq. (3) is also suitable for a TL pulse.

The idea originates from the phase function of a Fresnel zone plate in the spatial domain, which can be given by [18]

$$\phi(r) = \exp\left(-\frac{i\pi r^2}{\lambda f}\right), \quad (5)$$

where λ and f are the wavelength of the incident light and the focal length of the zone plate, respectively. According to the partition method of the Fresnel zone plate, the radius of the kth zone is

$$\rho_k = \sqrt{k\lambda f}. \quad (6)$$

Similarly, the width of the nth frequency zone in Eq. (3) can be rewritten as

$$\Omega_n = \sqrt{[4n(1-1/4n)\pi]/2\alpha} = \sqrt{k'\lambda' f'} \ (n = 1,2,3\ldots). \quad (7)$$

Hence, we can obtain $k' = 4n$ and $\lambda' f' = [(1-1/4n)\pi]/2\alpha$. By analogy with Eq. (5), the phase function of the FIBPS in the frequency domain can be expressed as

$$\phi(\omega) = \exp\left(-\frac{i\pi\omega^2}{\lambda' f'}\right) = \exp\left[-\frac{i2\alpha\omega^2}{(1-1/4n)}\right]. \quad (8)$$

We can see from Eq. (8) that the FIBPS can introduce a negative frequency-dependent quadratic phase factor of -2α (negative chirp) for a TL pulse when the frequency zone n tends to infinity in theory, which is analogous to creating a Fresnel lens. Conversely, a chirped pulse with a chirp parameter of 2α can be compensated and translated into a TL pulse by shaping its spectrum with FIBPS, which has recently been realized experimentally [19]. In the practical experiment, one can achieve the above goal as long as n is sufficiently large, e.g., $n = 20$. In our previous theoretical work, a chirp pulse with the chirp parameter α was used as the FP. After compensating with FIBPS, the pulse is still chirped but with a negative chirp parameter $-\alpha$ which will not affect the final compression result. Thus, Eqs. (3) and (4) are also valid for a TL pulse and will lead to the same compression result as for a chirped pulse; the compression result is independent of the shape of the FP spectrum. Previous theoretical work [15,16] can also be explained and covered by the current analysis. Thus far, we have developed a comprehensive theory of FIBPS for the spectral compression of SHG whenever the FP spectrum is Gaussian or square, a TL pulse or not. In the subsequent section, as an example, we will experimentally verify the SHG spectral compression for a

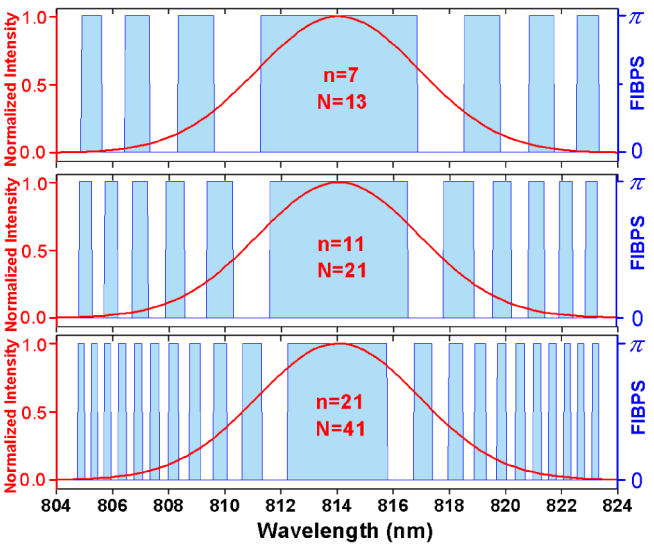

FIG. 1. Shaping scheme for a Gaussian pulse with FIBPS for n = 7, 11, and 21, respectively.

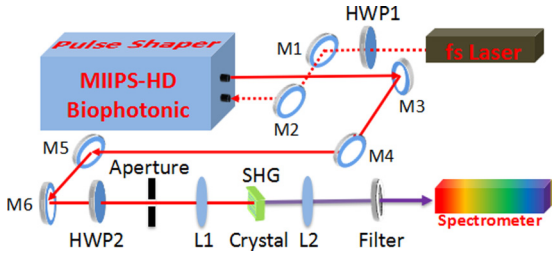

FIG. 2. Experimental setup. L: lens, HWP: half-wave plate, M: mirror.

TL pulse by shaping a Gaussian FP spectrum with FIBPS. For convenience, we will use the above formula with wavelength instead of frequency. The shaping scheme used in our experiment is shown in Fig. 1, where the Gaussian FP spectra are shaped with FIBPS for $n = 7$, 11, and 21, respectively.

III. EXPERIMENTAL RESULTS

A. Experimental setup

The experimental setup is illustrated in Fig. 2. A commercial Ti:sapphire laser (Fusion 100–1200, FEMTOLASERS) centered at 814 nm with a 3-dB bandwidth of 7 nm, pulse duration of 135 fs, and repetition rate of 75 MHz is used as the FP. After being collimated by a pair of lenses, the beam is input into a 4-f Fourier pulse-shaping system (MIIPS-HD, Biophotonic). A half-wave plate HWP1 is used to rotate the polarization of the input pulse field to obtain maximum diffraction efficiency when the light passes through the polarization-dependent grating. A reflection-type liquid crystal on a silicon spatial light modulator (LCOS-SLM, X10468-2, Hamamatsu) with 792 pixels is placed on the Fourier plane. The different frequencies in the input pulse are scattered in space by the grating and then enter the SLM after being collimated by a cylindrical lens. The shaped pulse is output above the incident pulse along the vertical direction and then arrives at HWP2 after being reflected four times, as shown in Fig. 2. Before the output shaped pulse is focused into 0.5-mm bismuth borate (BIBO) crystal for SHG, we use an aperture to block the unwanted zero-order diffracted light from first-order diffracted light, and HWP2 is used to optimize the SHG efficiency. The generated SHG signal is focused and then sent into the spectrometer (HR4000, Ocean Optics Inc., resolution of 0.02 nm) after filtering the residual FP light. A more detailed description of the experimental setup can be found in our recent publication [20].

The correspondence between the wavelength and pixels is calibrated with the pulse shaper by measuring the FP spectrum before the experiment. To determine the phase of the pulse before it enters the pulse shaper, phase compensation is performed on the input pulse, and its phase information is obtained using the MIIPS method [9,20]. In the following experiments, both FIBPS and the compensated phases of the input pulse are introduced by the SLM, and the desired phase functions can be written in the computer to control the phase of pixels in SLM.

B. Results

Figure 3 presents the results of SHG spectral compression by shaping the FP spectrum with FIBPS for (a) $n = 7$ ($N = 13$), (b) $n = 11$ ($N = 21$), and (c) $n = 21$ ($N = 41$),

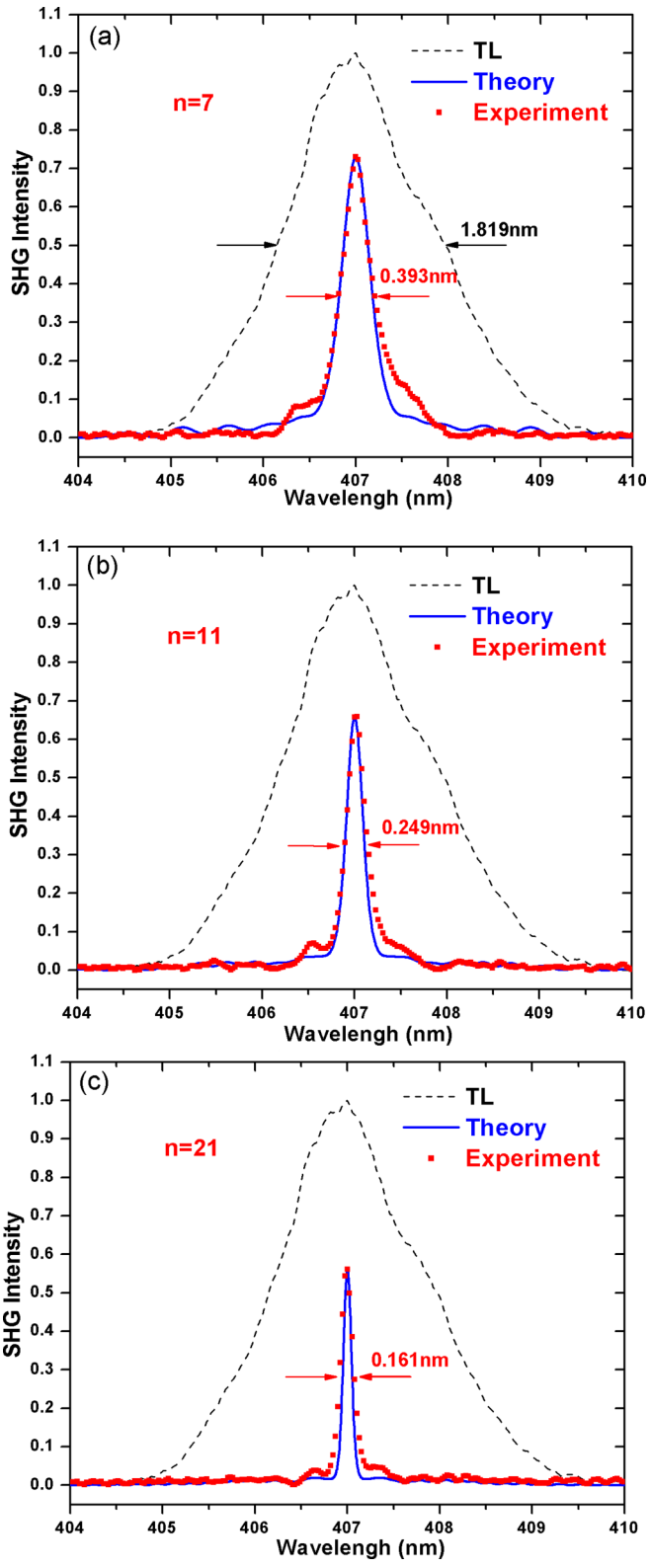

FIG. 3. SHG spectral compression with a 0.5-mm BIBO crystal for $n = 7$ (a), $n = 11$ (b), and $n = 21$ (c). The blue solid lines and red square points denote the theoretical and experimental results, respectively. The SHG spectrum has been normalized with respect to the TL SHG intensity (dashed lines).

respectively. The SHG spectrum has been normalized with respect to the TL SHG intensity (the dashed line) for

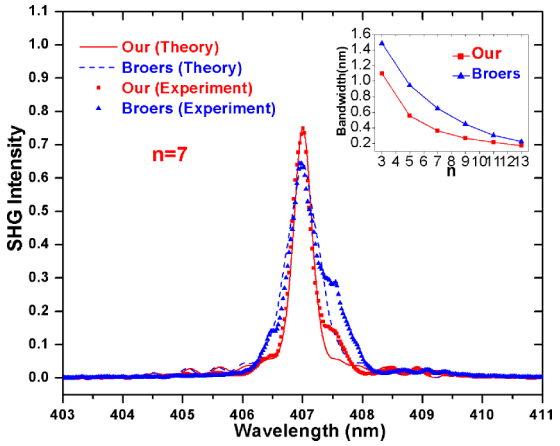

FIG. 4. Comparison of our SHG compressed results (red) to Broers's (blue) with a 10-μm beta barium borate (BBO) crystal for $n = 7$. The lines and points denote the theoretical and experimental results, respectively. The inset shows a comparison of compressed bandwidth (FWHM) versus n.

comparison. The compressed bandwidth FWHMs in the experiment are 0.393 nm, 0.249 nm, and 0.161 nm, respectively, while the peak intensities are about 73%, 66%, and 56%, respectively, compared to the TL SHG intensity. In addition, we have evaluated the overall intensities of the compressed SHG pulse relative to that of the TL SHG pulse, and ratios of 21%, 14%, and 9% have been achieved for $n = 7$, 11, and 21, respectively. Compared with the TL SHG spectral bandwidth of 1.819 nm, Fig. 3(c) shows a compression factor of 11.3 in our best case. The theoretical prediction for the spectral compression was also implemented. In the experiment, the TL FP has a full width (FW) of $\Delta\lambda_{\mathrm{FW}} = 18.674$ nm, from 804.648 to 823.322 nm ($\Delta\omega = 5.315 \times 10^{13}$ rad/s). The chirp parameters corresponding to $n = 7$, 11, and 21 are $2\alpha_1 = 30023\,\mathrm{fs}^2$, $2\alpha_2 = 47815\,\mathrm{fs}^2$, and $2\alpha_3 = 92293\,\mathrm{fs}^2$, respectively. The theoretical predictions for these three shaping cases were plotted by blue solid lines in Fig. 3, and very good agreements with the experimental results have been achieved.

C. Experimental comparison of our method to Broers's

To verify the superiority of our method, we also applied the Broers method for spectral compression and made a comparison with our method in the experiment. The results are shown in Fig. 4. The lines and points represent the theoretical and experimental results with our method (red) and that of Broers (blue) for $n = 7$ ($N = 13$, as an example), respectively. The experimental results show good agreement with the theory. It can be seen that the compressed bandwidth (FWHM) based on our method was 0.368 nm with a peak intensity of 75% compared to the TL SHG intensity, while with Broers's method, the compressed bandwidth was 0.587 nm with a peak intensity of 64%. It clearly verifies that our method is superior to that of Broers. The reason is that our method provides more exact phase relations between the different frequency components within the FP. The comparison of the compressed bandwidths between the two methods as a function of n is shown in the inset of Fig. 4. One can see that the superiority is evident when n is small. However, with the increase in n, the difference of the compressed bandwidth will tend to converge.

IV. DISCUSSION

As shown in Figs. 3 and 4, there are minor discrepancies between the experimental results and the theory, mainly on both sides. Such discrepancies can be attributed to the following factors: (1) Although the use of the MIIPS method can compensate for the majority of phases of the input pulse, there remains a small residual uncompensated phase, resulting in experimental errors. (2) The BPS we designed does not exactly coincide with the pixels in the SLM because of the limitation of the resolution of this pulse shaper, and this noncorrespondence will become more distinct when N increases. This is also one of the main reasons why the compression intensity decreases with n in Fig. 3. We also implemented the SHG spectral compression experiment for $n = 31$ ($N = 61$, not given in the text), where the obtained SHG intensity was lower and the compression bandwidth was even slightly larger than that for $n = 21$, indicating that the noncorrespondence between the phase shaping point and SLM pixels has become evident. We believe this error can be gradually eliminated with the improvement in SLM manufacturing technology and pulse shaper resolution. (3) The pixels in the SLM are discrete, and there is a gap (0.4 μm) between adjacent pixels. Since the light field passing through these gaps is not modulated (∼2%), this part of the energy will be lost, affecting the compression effect. In a practical experiment, as the shaper resolution is limited, it is necessary to choose a reasonable N to obtain a satisfactory compression effect.

It should be noted that binary amplitude modulation [2] can also be applied for spectral compression, while the compression effects of SHG spectrum will be worse with a broader bandwidth, lower intensity, and larger background [15]. Additionally, although we demonstrated the spectral compression of SHG for a Gaussian pulse, FIBPS is independent of the shape of the FP spectrum and it is suitable for a variety of commonly used pulses such as Gaussian, square, Lorentz, and hyperbolic secant. This is because FIBPS originates from the quadratic phase factor in Eq. (2) and is not related to the spectral amplitude. Moreover, based on the theoretical analysis, FIBPS can introduce a negative frequency-dependent quadratic phase factor (negative chirp) for a TL pulse; thus, it is not necessary that the FP be chirped. If a pulse is not a quadratic-phase chirped pulse but has an arbitrary phase, we can compensate the phase and translate it into a TL pulse by the MIIPS method in principle before a compression experiment. Thus, FIBPS provides a general method and can not only realize the spectral compression of SHG, but also be applied for solving other problems related to the dispersion compensation, such as chirped light pulse compression [19] and the compression of chirped biphotons [21]. According to Eq. (3), the chirp parameter related to the size of the dispersion is proportional to n for a given spectral bandwidth of the FP. Thus, our method can be very convenient to match the required amount of dispersion by only adjusting n. Note that because n takes a positive integer, the compensation is discrete.

We also implemented the experiment of SHG spectral compression with a 10-μm beta barium borate (BBO) crystal

for $n = 11, 21$ (not given in the text) and obtained the same compression effects. However, the compressed bandwidth in a short crystal will be broader than in a long crystal owing to the broadening of the phase-matching bandwidth. Furthermore, the SHG intensity obtained in a long crystal is higher than that in a short one because the SHG power scales linearly with the crystal length [3]. Therefore, in practical applications, longer crystals should be selected as the SHG crystal to obtain a narrower bandwidth with a high signal intensity.

V. CONCLUSION

We have extended the theory of FIBPS for spectral compression of SHG to a TL pulse with any symmetrical spectral shape and experimentally verified it for a Gaussian TL pulse as an example. For a given FP spectral bandwidth, a narrower bandwidth can be obtained in principle by simply increasing the total number of binary phases N while requiring a higher shaper resolution. The experiment also verified that our method is superior to that of Broers. Our method provides deterministic BPS with a small amount of binary phase sequences for effectively realizing SHG spectral compression without search space maps or any complex algorithms. These results will be useful in the applications of selective two-photon microscopy [7], two-photon imaging through biological tissue [11], and high-precision nonlinear spectroscopy [1,12]. Furthermore, FIBPS can be analogous to a Fresnel lens; thus it can introduce negative dispersion and can also be generalized to applications in the field of dispersion compensation, such as chirped pulse compression and the compression of chirped biphotons. Our work paves the way for exploring the applications of FIBPS to other fields involving a frequency-dependent quadratic phase factor, such as nonlinear spectroscopy, ultrafast optics, and quantum optics.

ACKNOWLEDGMENTS

This work was supported by the National Natural Science Foundation of China (Grants No. 11504292, No. 91336108, No. 11273024, No. 91636101, and No. Y133ZK1101), the Research Equipment Development Project of Chinese Academy of Sciences (Project Name: Quantum Optimization Time Transfer Experiment System Based on Femtosecond Optical Frequency Combs), the national youth talent support program of China (Grant No. [2013]33), the Frontier Science Key Research Project of Chinese Academy of Sciences (Grant No. QYZDB-SSW-SLH007), and Natural Science Basic Research Plan in Shaanxi Province of China (Grant No. 2016JQ1036).

[1] Y. Silberberg, Annu. Rev. Phys. Chem. **60**, 277 (2009).
[2] B. Broers, L. D. Noordam, and H. B. van Linden van denHeuvell, Phys. Rev. A **46**, 2749 (1992).
[3] Z. Zheng and A. M. Weiner, Opt. Lett. **25**, 984 (2000).
[4] Z. Zheng and A. M. Weiner, Chem. Phys. **267**, 161 (2001).
[5] K. A. Walowicz, I. Pastirk, V. V. Lozovoy, and M. Dantus, J. Phys. Chem. A **106**, 9369 (2002).
[6] V. V. Lozovoy, I. Pastirk, K. A. Walowicz, and M. Dantus, J. Chem. Phys. **118**, 3187 (2003).
[7] I. Pastirk, J. D. Cruz, K. Walowicz, V. V. Lozovoy, and M. Dantus, Opt. Express **11**, 1695 (2003).
[8] J. M. D. Cruz, I. Pastirk, V. V. Lozovoy, K. A. Walowicz, and M. Dantus, J. Phys. Chem. A **108**, 53 (2004).
[9] V. V. Lozovoy, I. Pastirk, and M. Dantus, Opt. Lett. **29**, 775 (2004).
[10] M. Comstock, V. V. Lozovoy, I. Pastirk, and M. Dantus, Opt. Express **12**, 1061 (2004).
[11] J. M. Dela Cruz, I. Pastirk, M. Comstock, and M. Dantus, Opt. Express **12**, 4144 (2004).
[12] V. V. Lozovoy, J. C. Shane, B. Xu, and M. Dantus, Opt. Express **13**, 10882 (2005).
[13] V. V. Lozovoy and M. Dantus, Chem. Phys. Chem. **6**, 1970 (2005).
[14] V. V. Lozovoy, B. Xu, J. C. Shane, and M. Dantus, Phys. Rev. A **74**, 041805(R) (2006).
[15] B. Li, Y. Xu, L. An, Q. Lin, H. Zhu, F. Lin, and Y. Li, Opt. Lett. **39**, 2443 (2014).
[16] B. Li, Y. Xu, H. Zhu, Q. Lin, L. An, F. Lin, and Y. Li, J. Opt. Soc. Am. B **31**, 2511 (2014).
[17] A. M. Weiner, Opt. Commun. **284**, 3669 (2011).
[18] A. Sakdinawat and Y. Liu, Opt. Lett. **32**, 2635 (2007).
[19] V. V. Lozovoy, M. Nairat, and M. Dantus, J. Opt. **19**, 105506 (2017).
[20] C. Zhou, B. Li, X. Xiang, S. Wang, R. Dong, T. Liu, and S. Zhang, Opt. Express **25**, 4038 (2017).
[21] B. Li, Y. Xu, H. Zhu, F. Lin, and Y. Li, Phys. Rev. A **91**, 023827 (2015).